Landscape Ecol (2021) 36:2565–2582
https://doi.org/10.1007/s10980-021-01281-z

RESEARCH ARTICLE

Landscape configuration of an Amazonian island-like ecosystem drives population structure and genetic diversity of a habitat-specialist bird

Camila D. Ritter · Camila C. Ribas · Juliana Menger · Sergio H. Borges · Christine D. Bacon · Jean P. Metzger · John Bates · Cintia Cornelius

Received: 24 December 2020 / Accepted: 9 June 2021 / Published online: 19 June 2021

Abstract

Context Amazonian white-sand ecosystems (*campinas*) are open vegetation patches which form a natural island-like system in a matrix of tropical rainforest. Due to a clear distinction from the surrounding matrix, the spatial characteristics of *campina* patches may affect the genetic diversity and composition of their specialized organisms, such as the small and endemic passerine *Elaenia ruficeps*.

Objectives To estimate the relative contribution of the current extension, configuration and geographical context of *campina* patches to the patterns of genetic diversity and population structure of *E. ruficeps*.

Methods We sampled individuals of *E. ruficeps* from three landscapes in central Amazonia with contrasting *campina* spatial distribution, from landscapes with large and connected patches to landscapes with small and isolated patches. We estimated population structure, genetic diversity, and contemporary and historical migration within and among the three landscapes and used landscape metrics as predictor variables.

Supplementary Information The online version contains supplementary material available at https://doi.org/10.1007/s10980-021-01281-z.

C. D. Ritter (✉)
Department of Eukaryotic Microbiology, University of Duisburg-Essen, Universitätsstrasse 5, 45141 Essen, Germany
e-mail: kmicaduarte@gmail.com

C. D. Ritter
Departamento de Zootecnia, Grupo Integrado de Aquicultura e Estudos Ambientais, Universidade Federal do Paraná, Rua dos Funcionários, 1540, Juvevê, Curitiba, PR 80035-050, Brazil

C. C. Ribas · J. Menger
Coordenação de Biodiversidade e Coleções Zoológicas, Instituto Nacional de Pesquisas da Amazônia, Av. André Araújo 2936, Manaus, AM 69060-001, Brazil

S. H. Borges · C. Cornelius
Instituto de Ciências Biológicas, Universidade Federal do Amazonas, Av. Rodrigo Otávio Jordão Ramos 3000, Bloco ICB01, Setor Sul, Manaus, AM 69077-000, Brazil

C. D. Bacon
Department of Biological and Environmental Sciences, University of Gothenburg, Box 463, 405 30 Göteborg, Sweden

C. D. Bacon
Gothenburg Global Biodiversity Centre, Box 461, 405 30 Göteborg, Sweden

J. P. Metzger
Departamento de Ecologia, Instituto de Biociências, Universidade de São Paulo, Rua do Matão, 321, travessa 14, São Paulo, SP 05508-900, Brazil

Furthermore, we estimated genetic isolation by distance and resistance within landscapes.

Results We identified three genetically distinct populations with asymmetrical gene flow among landscapes and a decreasing migration rate with distance. Within each landscape, we found low differentiation without genetic isolation by distance nor by resistance. In contrast, we found differentiation and spatial correlation between landscapes.

Conclusions Together with previous studies, the population dynamics of *E. ruficeps* suggests that both regional context and landscape structure shape the connectivity among populations of *campina* specialist birds. Also, the spatial distribution of Amazonian landscapes, together with their associated biota, has changed in response to climatic changes in the Late Pleistocene.

Keywords *Campinas* · *Elaenia ruficeps* · Landscape genetics · Migration · Spatial isolation

Introduction

Landscapes are mosaics of environments with distinct structure and biotic composition. Natural island-like systems such as habitat patches, caves, and mountaintops provide important contributions to landscape structure and diversity (Itescu 2019). Due to their well-defined borders and distinction from the surrounding habitats, the spatial characteristics of island-like systems may influence biological assemblages and their attributes including the genetic diversity and differentiation. These island-like systems can vary in the extent of insularity they impose on the taxa they harbor, affecting the extent to which organisms can disperse and colonize new patches (Itescu 2019). Furthermore, island-like systems contribute for a higher beta-diversity in several natural ecosystems such as tropical forests (Draper et al. 2018).

Amazonia has the highest biodiversity among all tropical rainforests and is a global biodiversity hotspot (Hansen et al. 2013). The predominant view of Amazonia as a homogeneous, humid tropical forest does not match the heterogeneity of landscapes it harbors (Myster 2016; Tuomisto et al. 2019). Indeed, Amazonia comprises diverse vegetation formations from humid tropical forests (*terra-firme*) to non-forested formations, such as white-sand grasslands and shrubby habitats occurring as an island-like system (Anderson 1981; Adeney et al. 2016; Capurucho et al. 2020a).

White-sand shrub and grassland patches, hereafter *campinas*, are naturally patchy and resemble islands in a "sea" of forests, growing on nutrient-poor soils (Prance 1996; Fine et al. 2010; Ritter et al. 2018; Capurucho et al. 2020a; Costa et al. 2020). *Campina* patches cover approximately 1.6% of the Amazon basin (Adeney et al. 2016), yet are an important Amazonian island-like system, harboring a unique biota (Borges et al. 2016a; Capurucho et al. 2020a; Costa et al. 2020). Landscapes with *campina* patches have different spatial configurations throughout Amazonia, composed of large and connected patches in the north and small and isolated patches in the south (Borges et al. 2016a).

Moreover, properties of *campina* landscapes, such as amount of habitat, patch isolation and matrix properties, vary across space and time. As such, it is expected that gene flow among populations and hence genetic diversity of populations inhabiting *campina* patches will depend on the structure of these landscapes. Thus, landscapes with more *campina* habitat cover and with connected patches should harbor a higher genetic diversity than landscapes with reduced habitat and isolated patches. However, the effects of landscape configuration on the organisms that thrive in naturally patchy *campinas* remain poorly understood (but see Capurucho et al. 2013; Borges et al. 2016a).

Several factors may restrict the movement of individuals in island-like systems, such as *campinas*. In naturally heterogeneous landscapes, restrictions of movement and gene flow can be due, for instance, to geographic distance (isolation by distance; Wright 1943), or to non-suitable habitat (isolation by resistance; e.g. McRae 2006; DiLeo and Wagner 2016). Dispersal may promote gene flow and connect geographically isolated populations, increases genetic diversity, and reduces inbreeding (Ronce 2007). However, dispersal through non-suitable habitats also represents high energetic costs and mortality risks (Fahrig 1998; Gruber and Henle 2008).

J. Bates
Life Sciences Section, Negaunee Integrative Research Center, The Field Museum of Natural History, 1400 S. Lake Shore Drive, Chicago, IL 60605, USA

The geographic distance between patches, within and among landscapes, and the type and configuration of environments in the matrix may affect the ability of a species to disperse (Bates 2002). Different matrices create variable resistance to individuals' movement (Itescu 2019). In Amazonia, white water rivers, such as the Amazon River, and the associated floodplains appear to impose large resistance for white-sand vegetation specialist birds (Capurucho et al. 2013; Matos et al. 2016; Ritter et al. 2021). However, little is known about how composition and configuration of *campina* landscapes shape movements of specialist species. Also, there is a long debate in the literature about how dynamic the spatial distribution of open and forested Amazonian landscapes have been during the Quaternary (Cheng et al. 2013; Wang et al. 2017; Rocha and Kaefer 2019). This historical dynamic may have affected movement patterns of individuals within and among landscapes over time (Manicacci et al. 1992), thus understanding these movements can potentially provide information on landscape configuration changes in the past.

Methods of molecular analyses have been successfully used to investigate patterns and to infer processes related to the origin and maintenance of biodiversity (e.g. Antonelli et al. 2018; Silva et al. 2019). The use of gene sequencing can reveal historical patterns through phylogeographic studies (Avise 2009). On the other hand, the genotyping of microsatellite markers can reveal contemporary patterns, because they are highly polymorphic due to their high mutational rate (Tautz 1989), and are therefore ideal for studies of contemporary population structure (Frankham et al. 2002). In this context, the use of molecular markers with distinct evolutionary rates may uncover how the interaction between landscape features and micro-evolutionary processes shapes patterns of genetic structure and diversity in time and space (Capurucho et al. 2013).

In this study we investigate the effects of landscape configuration on population genetic structure and diversity in a white-sand vegetation specialist bird species restricted to Amazonian *campina* patches, *Elaenia ruficeps* (Aves: Tyrannidae; Rheindt et al. 2008; Borges et al. 2016b), employing mitochondrial gene sequences and microsatellite markers. We address the following questions: (1) How do genetic diversity, population structure, and migration rates differ within and among three *campina* landscapes with contrasting configuration? We expect differences between genetic metrics measured through markers with faster (microsatellites) and slower (DNA mitochondrial sequences) evolutionary rates that responded to processes at different time scales, with microsatellite markers reflecting current and mtDNA historical landscape structure. (2) How do the amount and isolation of habitat patches within and among landscapes affect population genetic diversity in *E. ruficeps?* We expect that both metrics will be important but habitat amount will be the strongest factor explaining genetic diversity. (3) What is the relative importance of geographical distance and matrix resistance in limiting gene flow in *E. ruficeps?* We expect that habitat matrix resistance will better explain genetic differentiation among populations when compared to geographic distance. We explicitly tested if *terra-firme forest* and rivers limited the movement of *E. ruficeps* individuals more than other landscape matrix types, such as seasonally flooded forests.

Materials and methods

Study area

We sampled birds in three landscapes (each *ca* 50 × 50 km) north of the Amazon River (Fig. 1A): Aracá (0°28′7.76″N, 63°28′32.20″W; Fig. 1B), Viruá (1°36′N, 61°13′W; Fig. 1C), and Uatumã (2°17′9.19″S, 58°51′53.92″W; Fig. 1D). The Aracá landscape lies on the eastern side of the middle part of the Negro River basin on the western margin of the Branco River (i.e. in the Branco-Negro interfluve) and has the highest *campina* vegetation coverage (45.33% of its area in 50 × 50 km^2) distributed as large and connected patches. The Viruá landscape is located on the eastern margin of the Branco River, and has intermediate *campina* vegetation coverage (28.2% of its area) distributed as both large and small interconnected patches. This is the only site with some anthropogenic disturbance due to an interstate road and a few secondary non-paved roads among the sampling sites. The third and southernmost landscape, Uatumã, is located on the banks of the Uatumã River, inside the limits of the Uatumã Sustainable Development Reserve. The Uatumã landscape has less *campinas* coverage (0.8% of its area) with small and isolated *campina* patches (Fig. 1B–D). We established

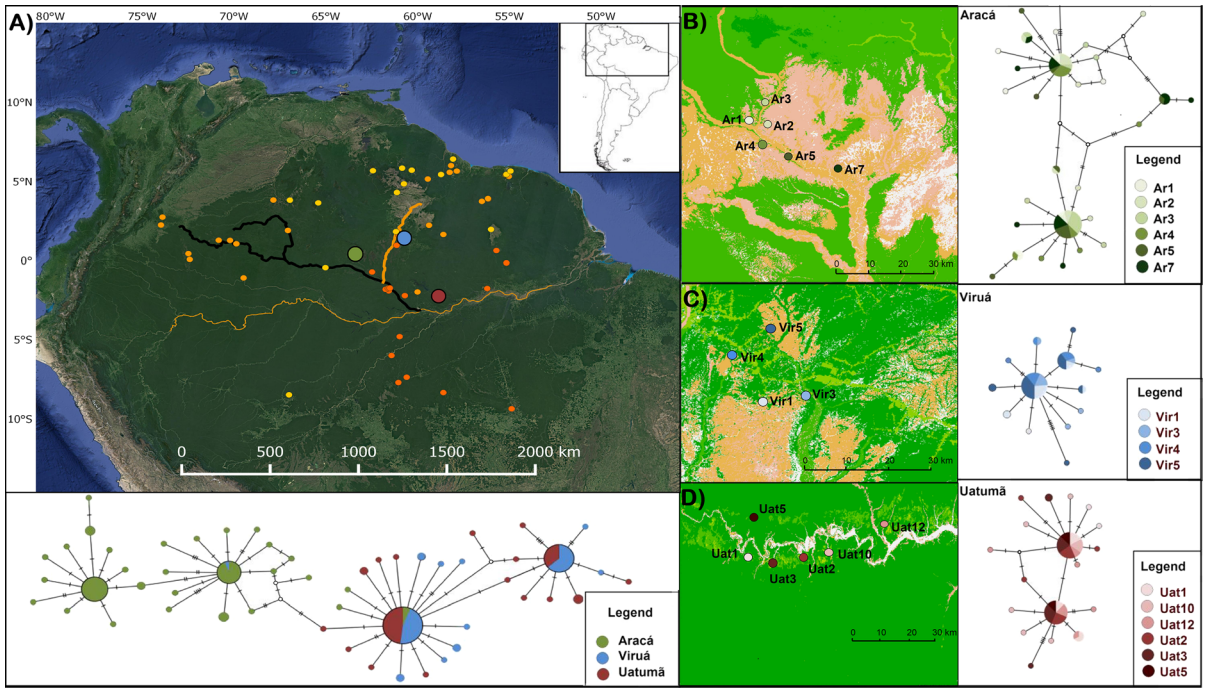

Fig. 1 **A** Map of the distribution of *Elaenia ruficeps*. Points in yellow are from the Global Biodiversity Information Facility (GBIF 2017) public database (general and potentially biased by mis-identification); points in bright orange are from museum collections (highly curated locality information). Points in dark orange are areas with available tissue samples. Points in green, blue, and red are the landscapes sampled in this study (Aracá, Viruá, and Uatumã respectively), with the respective haplotype network below the map. The main rivers of the Amazon basin are shown according to their water color; rivers with high sediment concentration are brown, with low sediment concentration are blue. We highlight the Negro River in black and the Branco River in brown both with tick lines. **B** shows in detail the sites sampled in Aracá with the respective haplotype network; **C** shows the sites sampled in Viruá with the respective haplotype network and; and **D** shows the sites sampled in Uatumã and the respective haplotype network. Map produced in QGIS v.3.6.2

six sampling sites within the Aracá landscape, six sampling sites within the Uatumã landscapes, and four sampling sites within the Viruá landscape, with a total of 16 sampling sites. These sites were distributed across landscapes in *campinas* vegetation with distances ranging from 5 to 44 km among them within landscapes, as described in Capurucho et al. (2013) and Borges et al. (2016a).

Landscape metrics

We used categorical maps with six pre-defined classes: *terra-firme forest*, *campinas*, *campinarana* (white-sand patches with taller vegetation coverage than *campinas*), flooded forest, water, and anthropogenic areas (see Capurucho et al. 2013 for details on the classification method). We used ArcGIS v.9.1 (Press 2005) and Fragstas v.3.4 (McGarigal et al. 2002) to calculate two landscape metrics. The first was a habitat amount metric calculated as the area of *campina* vegetation in a radius of 5 km around each sampling site. As a configuration metric, we used the proximity index, an isolation measure of each patch in which sampling sites were located, that was based on the sum of the area of neighboring patches within a 5 km search radius, weighted by the distance to neighboring patches (Gustafson and Parker 1994). The 5 km radius was selected based on dispersal kernels described for several Neotropical bird species; most Amazonian birds disperse less than 5 km (Van Houtan et al. 2007). The minimum distance among sites was 5 km, but most sites (> 85%) were more than 10 km apart (with only two pairs of sites 5 km apart, one pair in Aracá and one in Virua, with other 3 pairs of sites close to 10 km apart). Therefore, overlap was minimal. Habitat amount and proximity index were not correlated (Pearson correlation = 0.3, p = 0.24).

Sampling

We defined sampling area as a 500 m radius circle centered at each sampling site, in which 20 mist-nets (12 m long, 36 mm mesh size) were equally distributed into four lines. In order to reduce the probability of sampling only one family group, at least two mist-net lines were moved each day to cover other parts of the sampling sites. Sampling was conducted during the dry season of 2010 and 2011, and each site was sampled as many days as needed to capture at least 10 individuals per site, ranging from 2 to 5 days per site, but in four sites the intended number of individuals was not attained (see Table S1). A blood sample ($\sim$ 50 µl) was taken from each captured individual, stored in ethanol, and deposited in the Genetic Resources Collection of the National Institute for Amazonian Research (INPA, Manaus, Brazil). Voucher specimens (maximum of five per landscape) were also collected and deposited at INPA Bird Collection.

DNA sequencing

DNA was extracted from blood or tissue samples using Promega DNA Purification Kit (A1125). The complete sequence of the mitochondrial NADH Dehydrogenase 2 (ND2) gene was amplified using the external primers L5204 and H6313 (Sorenson et al. 1999). For this study, we also designed a primer for reverse gene sequencing (H6242; 5'-TAGGATTGTAGGGGATAAAGGTA-3 ') that is internal for ND2 gene, because some samples did not amplify well with H6313. Amplification and sequencing details are described in Capurucho et al. (2013). Contiguous sequences were assembled and aligned in Geneious v. 5.6.5 (Biomatters 2012).

Microsatellite genotyping

All individuals of *E. ruficeps* were genotyped at 15 microsatellite loci described in Ritter et al. (2014), using protocols and PCR conditions therein (Table S2). We did not use the Eru7 and Eru8 loci because they failed for several samples in our genotyping. PCR products were run on an ABI PRISM 3730 DNA Analyzer; size scoring was performed with GeneMarker® v2.2.0 (Hulce et al. 2011). We calculated the number of alleles per locus, deviations from Hardy–Weinberg equilibrium (HWE), and linkage disequilibrium between pairs of loci for the three landscapes using Genepop Web v.4.2 (Raymond and Rousset 1995; Rousset 2008; Table S2). We also calculated the observed and expected heterozygosity (H_o and H_s) and allelic richness per loci for the three landscapes using the *hierfstat* v.0.4.22 R package (Goudet and Jombart 2015) in R v.3.2.5 (R Core Team 2015).

Genetic diversity, population structure, and migration rates

To investigate if genetic diversity varies within and among landscapes, we calculated four genetic diversity metrics (two based on mitochondrial and two on microsatellite data). For each locality (both landscapes and sites within each landscape), we estimated the individuals nucleotide diversity (P_i) and haplotype diversity (H_D) based on ND2 mitochondrial sequences using DnaSP v.5.10.01 (Librado and Rozas 2009). For the microsatellite data, we estimated allelic richness per site and per landscape using the rarefaction method implemented in the *PopGenReport* v.2.2.2 R package (Adamack and Gruber 2014) in R, and calculated the microsatellite genetic diversity (Theta) using Arlequin v.3.11 (Excoffier et al. 2005).

To describe historical population structure within and among landscapes, we constructed haplotype networks with ND2 sequences, with all individuals together and for individuals from each landscape separately, using a minimum spanning network (Clement et al. 2002) with Popart v.1.7 (Leigh and Bryant 2015). We used BAPS v.6.0 (Bayesian Analysis of Population Structure; (Corander et al. 2013) to infer the number of clusters (K) based on the mitochondrial data using all individuals. Likelihood values of the mixture analysis were calculated three times for each number K of subpopulations, ranging from 1 to 20 (since the number of sites was 16 and we expected no more than 20 population), accepting the partition with K value with higher likelihood, which were run until achieving convergence.

To describe current population structure within and among landscapes, we used microsatellite data. We used Structure v.2.3.4 (Pritchard et al. 2000) to infer the number of genetically distinct populations (K). We assumed an admixture model with correlated allele frequencies and the LOCPRIOR model (Hubisz et al.

2009). We used two LOCPRIOR options, first, we made analyses at the landscape level, with Aracá, Viruá and Uatumã as localities. Secondly, we analyzed the data using each sampling site as unique localities (16 in total). To identify the best estimate of *K* from 1 to 20 (both sampling sites as populations and landscapes as populations), we set a burn-in period of 100,000 followed by additional 1,000,000 iterations, and 20 replicates were run at each *K*. We determined *K* based on the log posterior probability of the data for a given *K* (Pritchard et al. 2000), and on the rate of change in the log probability of the data between successive clusters—the ΔK statistic (Evanno et al. 2005). These analyses were performed in Structure Harvester v.0.6.94 (Earl 2012). All runs were averaged at the best *K* with Clumpp v.1.1.2 (Jakobsson and Rosenberg 2007) and results were visualized with Distruct v.1.1 (Rosenberg 2004).

We inferred historical migration rates using mitochondrial sequences in Migrate-N v.3.6 (Beerli 2009). Under a coalescent framework and the infinite allele model, Migrate-N estimates migration rates (measured as a mutation-scaled immigration rate, M) up to $\sim$ 4 effective population size (Ne) generations (thousands of years). We used slice sampling to run four statistically heated parallel chains (heated at 1.0, 1.5, 3.0, and 1,000,000) for 1,000,000 iterations, and excluded 100,000 iterations as burn-in. MCMC estimates of M were modeled with prior boundaries of 0 and 100,000. We used a full migration model and considered parameter estimates accurate when an effective sample size (ESS) > 1000 was observed (Converse et al. 2015). We multiplied M by the mutation rate, $0.0105*10^{-4}$ for the mitochondrial data (Lovette 2004; Weir and Schluter 2008). To test for spatial auto-correlation of migration rate, we performed a Mantel test with pairwise migration rates and geographic distances (Euclidean) using the *vegan* v. 2.4-3 (Oksanen et al. 2010) R package. We performed these analyses between landscapes.

To estimate current migration rates, we used the microsatellite data in BayesAss v.3.0 (Wilson and Rannala 2003), which applies a Bayesian approach and MCMC sampling to estimate migration (m) over the last few generations. This analysis was run with 10 million iterations, a sampling frequency of 2000, a burn-in of 10%, and default settings. We estimated the migration rate between the three landscapes.

To identify if past demographic changes explain genetic diversity and migration rates, we inferred historical population demography using a Bayesian coalescent skyline plot (Drummond et al. 2005) as implemented in Beast v.1.8.2 (Drummond et al. 2012). We chose the most suitable substitution model for the mitochondrial data based on Bayesian information criterion (BIC) with jModelTest2 v.2.1.10 (Darriba et al. 2012). We set the substitution model chosen by jModelTest2 (HKY+ invariable sites) under a strict-clock model and the general avian substitution rate of mitochondrial evolution of 2.1% sequence divergence per million years (Lovette 2004; Weir and Schluter 2008). Runs of 100 million steps were performed, sampling every 10,000 steps under default settings. Skyline plots were constructed using Tracer v.1.6 (Rambaut and Drummond 2007). We reconstructed historical population size considering all populations together and then separately for Aracá and for Viruá + Uatumã following the populations identified with BAPS.

Landscape metrics and genetic diversity

To investigate if landscape metrics predict genetic diversity metrics, we calculated genetic metrics through nucleotide diversity (P_i) and haplotype diversity (H_D) from mitochondrial sequences and allelic richness (A_R) and genetic diversity (Theta) from microsatellite data. We calculated these metrics within each site and analyzed them as a function of the two landscape metrics (habitat amount and proximity index) and of the landscape of origin of each site (Aracá, Viruá or Uatumã).

For each dependent variable (P_i, H_D, Theta, and A_R), we defined a set of models to explain variation in genetic diversity. The final model set included models for each single landscape metric, and additional models with additive and interaction terms of the landscape origin to determine whether landscape context was also an important factor (i.e. to which landscape each group of sampling sites belongs to). The final model set also included a constant, intercept-only model, comprising a total of seven models for each dependent variable (Table S3).

Models were selected using an information theory approach based on AIC (Akaike 1974) and using the corrected AIC (AICc) for small sample sizes (Burnham and Anderson 2002). Models with $\Delta AIC \leq 2$

were considered equally plausible and we used the normalized model weight (AICw) to contrast the best model to the constant (no-effect) model. We used generalized linear models (Crawley 2013) with Gaussian error distribution after checking for the distribution of residuals. Before running the analysis landscape metrics were standardized to mean = 0 and variance = 1 to make different metrics comparable. The GLM analyses were performed using the *vegan* v. 2.4-3 (Oksanen et al. 2010) package and the model selection was made using the *bbmle* v.1.0.20 (Bolker and Bolker 2017) package, both in R.

Geographic isolation by distance and by resistance

To determine if genetic differentiation is better predicted by geographic distance or resistance we calculated the pairwise genetic differentiation F_{ST} (Weir and Cockerham 1984) for both mitochondrial and microsatellite data between landscapes and among sites within landscapes separately using the *fstat* function in the *hierfstat*, with 1000 permutations to obtain significance (Goudet 2001). To investigate patterns of isolation by geographical distance, we performed Mantel tests also in *vegan*. We used a pairwise geographic (Euclidean) and a pairwise genetic distance (F_{ST} values). We performed these analyses both between landscapes and between sampling sites within each landscape separately.

To investigate the patterns of isolation by resistance we assigned resistance values to vegetation cover within each landscape based on a questionnaire given to four expert Amazonian ornithologists for each landscape category for *E. ruficeps* (Table S3). Values ranged from 0.01 (less resistance) to 0.99 (more resistance). We took the average resistance value of each landscape category to calculate the isolation by resistance (Table S3). We used the *gdistance* v. 1.2-2 (Etten 2017) R package to create the transition layer using the inverse of the sum of each pixel to create the conductance layer (Fig. S1) and the *commuteDistance* function that calculates the expected random-walk commute resistance between nodes in a graph, to create the pairwise resistance matrix for each landscape. We then performed a Mantel test using the pairwise genetic distance (F_{ST} values) against the resistance distance. Additionally, we calculated the minimum resistance distance (i.e., least cost path) for each pair of sites and a Mantel test with the pairwise genetic distances (F_{ST} values).

Results

Genetic diversity, structure, and migration

We obtained 978 bp of the ND2 gene for 178 individuals, with 62 variable sites. Haplotype diversity from mitochondrial data of all samples was 0.79 (± 0.08 standard deviation [sd]) and nucleotide diversity was 0.002 (± 0.001 sd). For microsatellite data, we scored the same 178 individuals at 15 loci. No departure of Hardy–Weinberg Equilibrium was detected at any locus and no pair of loci was in linkage disequilibrium (see Table S2 for number of alleles per locus). Aracá landscape had the highest haplotype (0.84 ± 0.07 sd) and nucleotide diversity (0.003 ± 0.0006 sd) for mitochondrial data. For microsatellite data Aracá also had the highest allelic richness (19.49 ± 15.65 sd) but Viruá had the highest genetic diversity (1.69 ± 0.04 sd, Table S4).

We detected low but significant genetic differentiation among landscapes for both mitochondrial and microsatellite data (Table 1). For mitochondrial data, Viruá and Aracá had the largest differentiation (F_{ST} = 0.1, $p < 0.05$), while the largest differentiation for microsatellite data was inferred between Viruá and the Uatumã landscapes (F_{ST} = 0.02, $p < 0.05$, Table 1). Comparing among all sampling sites, within and among landscapes, mitochondrial results revealed low but significant differentiation among almost all sites within each landscape. Only seven comparisons with mtDNA are not significant, all of which are within landscapes (six in Aracá and one in Uatumã; Table S5), none are between landscapes. Values of

Table 1 F_{ST} among landscapes

	Arcacá	Uatumã	Viruá
Aracá	–	0.0194	0.0102
Uatumã	0.09732	–	0.0201
Viruá	0.10579	0.00507	–

Values above the diagonal are microsatellite F_{ST} and below the diagonal are ND2 sequence F_{ST}. All values are significant at $P < 0.05$

F_{ST} are lower between Viruá and Uatumã. Genetic differentiation among sites from different landscapes was higher than among sites within landscapes and in most cases significant, except between some Uatumã and Viruá sites (Table S5). Microsatellite results revealed several cases of non-significant differentiation among sites, within and among landscapes (Table S5). For sites in different landscapes, the sites from Uatumã were more differentiated than sites of both Aracá and Viruá (Table S5).

We found 56 mitochondrial haplotypes that grouped into three main clusters. Most haplotypes from the Aracá landscape were not shared with the Viruá and Uatumã landscapes, and within Aracá the haplotypes were grouped in two main clusters. Only one Aracá haplotype (from two individuals) was shared with the other two landscapes, and two additional Aracá haplotypes cluster with the Viruá and Uatumã samples (Fig. 1A). Despite clear differentiation between Aracá and the other two landscapes, the haplotype networks inside each landscape had little or no small-scale geographic structuring. Within each landscape, sampled haplotypes occurred in almost all sampled sites (Fig. 1B–D). BAPS results agree with the haplotype networks and inferred $K = 3$ populations, with two groups within Aracá and one with all haplotypes from Viruá and Uatumã, including three Aracá haplotypes found in five individuals (Fig. 2A), log (marginal likelihood) of optimal partition = − 920.3443, 1.00 probability of K = 3. For microsatellites, the highest log posterior probability of the data and the highest value for ΔK obtained via Structure analysis also inferred $K = 3$ (Fig. 2B), however the populations recovered by the microsatellite data corresponded to the three sampled landscapes.

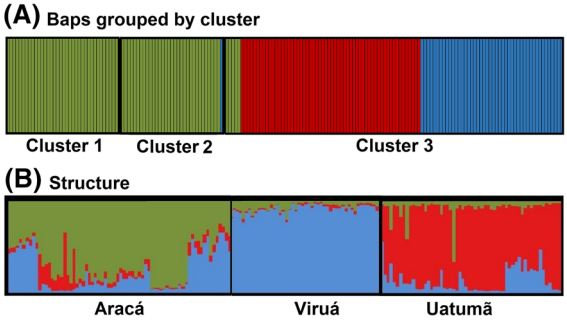

Fig. 2 Population structure of *Elaenia ruficeps* based on **A** mtDNA (BAPS) with individuals ordered by cluster membership and colored by landscape of origin (landscapes in decreasing order of *campina* habitat coverage: Aracá = green, Viruá = blue, Uatumã = red), and **B** Microsatelites (Structure), for which clusters match the different landscapes. In both analyses recorded $K = 3$ genetic clusters, which are delimited by thick black lines

Estimates of historical migration obtained from Migrate-N with mitochondrial data indicated low and asymmetrical gene flow from Uatumã to Viruá (0.0009) and from Viruá to Uatumã (0.0003), with even lower but symmetrical rates between Viruá and Aracá (0.0001 in both directions), and very low rates between Uatumã and Aracá (< 0.00006 in both directions; Fig. 3A). Estimates of contemporary migration obtained from BayesAss with microsatellite data resulted in high self-recruitment rates for all three landscapes (Aracá = 0.99 [± 0.006], Uatumã = 0.67 [± 0.005] and Viruá = 0.67 [± 0.006]). Contemporary migration was also asymmetrical, with individuals moving mainly from Uatumã and Viruá towards Aracá, 0.32 (± 0.008) and 0.32 (± 0.009), respectively (Fig. 3B). Among all sites, historical ($r = 0$, $p = 0.5$) and contemporary ($r = -0.08$, $p = 0.84$) migration rates were not related with geographic distance (Fig. S2A). Also, among landscapes, contemporary ($r = -0.03$, $p = 0.67$) and historical ($r = 0.16$, $p = 0.67$) migration rates were not significantly related to geographical distance (Fig S2B).

Finally, based on the Bayesian skyline plot we could infer the historical processes for the later Pleistocene (around 0.1 mya), with specifically more accuracy around 0.05 mya (Fig. S3). Analyses based on the mitochondrial data showed demographic expansion for *E. ruficeps* population as a whole. Bayesian skyline plot estimates showed general population expansion over the last 50,000 years (Fig. S3A). When we estimated demography separately, following BAPS clusters, the Aracá population showed demographic expansion over the last 50,000 years (Fig. S3B), but the Viruá and Uatumã populations maintained their population size constant over time (Fig. S3C).

Landscape metrics and genetic diversity

For the nucleotide diversity metric (Pi), a single best model was selected that contained landscape of origin as the single predictor variable (AICw = 0.7686), while for haplotype diversity (H_D) the single best model was the constant intercept-only model (AICw = 0.5573). For microsatellite genetic diversity (Theta),

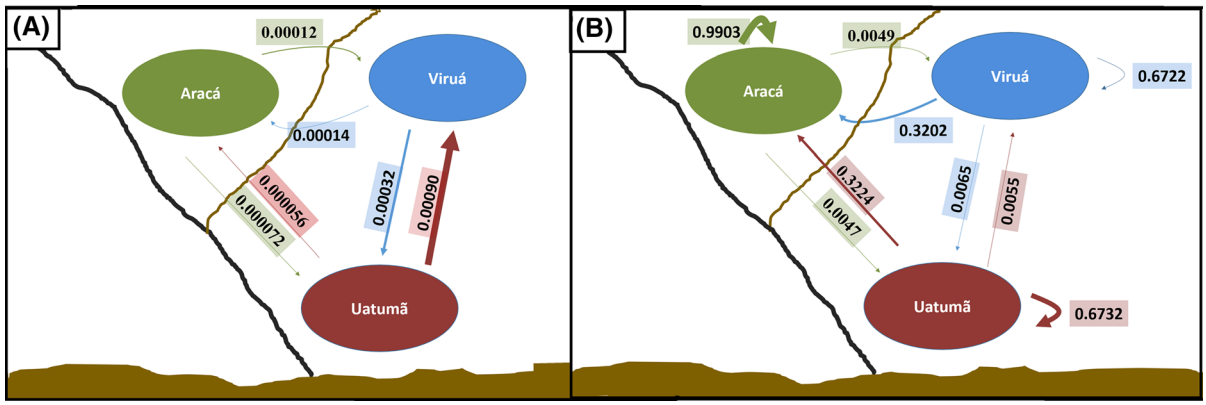

Fig. 3 Pairwise migration rates. **A** Historical migration rate calculated for mtDNA ND2 sequences in Migrate-N. **B** Contemporary migration rate calculated in BayesAss using microsatellite data. The size of the arrows is proportional to the migration estimates. Black line represents Negro River and brown line the Branco River. Brown coloration in the bottom of the figure represents the Amazon River. Historical migration shows the highest migration rate between Uatumã and Viruá, while contemporary migration shows higher self-recruitment with migration from Uatumã and Viruá to Aracá

a single best model was selected that contained just landscape of origin as predictor variable (AICw = 0.732) and for allelic richness (A_R) the single best model contained de proximity index as the single best predictor variable (AICw = 0.9376, Fig. 4A–D). See respective ΔAICc and AIC weights in Table 2 and best models estimated parameters in Table S6.

Geographical distance, resistance and gene flow

Genetic distance (F_{ST}), for both microsatellite (r = 0.41, p = 0.01) and mitochondrial (r = 0.48, p = 0.001) data, was positively correlated with geographic distance among landscapes (Fig. 5A, B). However, no correlation with geographic distance was found among sites within each landscape (Table S8; Fig. 5C, D). No significant relationship was found between genetic differentiation (F_{ST}) and resistance between sites within each landscape, in either dataset (mitochondrial or microsatellite) using the random-walk commute resistance (Table S8; Fig. 5E, F) or the pairwise minimal resistance between the sites.

Discussion

We used molecular markers with different evolutionary rates to determine patterns of genetic diversity and population structure of *Elaenia ruficeps*, a white-sand specialist bird, by sampling three landscapes with different amount of habitat and configuration of *campina* patches in central Amazonia. We found that: (1) landscapes harbor genetically distinct populations, with asymmetrical gene flow among them; (2) historical and contemporary estimates of genetic structure and migration rates differ, implying dynamic connections among landscapes through time; (3) overall genetic structure (diversity and differentiation) is best explained by a regional effect (i.e. landscape of origin), than by habitat configuration, except for allelic richness which increases with patch proximity (more connectivity), supporting some evidence for local movement restriction between isolated patches; and (4) genetic differentiation increases with geographical distance among landscapes, whereas within landscapes no isolation by distance or by resistance is detected although low genetic differentiation is detected among patches. Taken together, our results suggest that although dispersal of *E. ruficeps* between *campina* patches is restricted to some degree locally, dispersal limitation is strong at regional scales (between landscapes), hampering gene flow. Thus, our results stress the high complexity in *E. ruficeps* population dynamics in habitats with insular nature.

A caveat of our analysis within landscapes may be the limited number of samples per site. To avoid biases of sample size, ideally we should have more than 25 individuals per site (Hale et al. 2012). This limitation could explain, in part, our lack of structure within landscapes since the F_{ST} showed low, but significant difference between most of the sites (Table S5). Also,

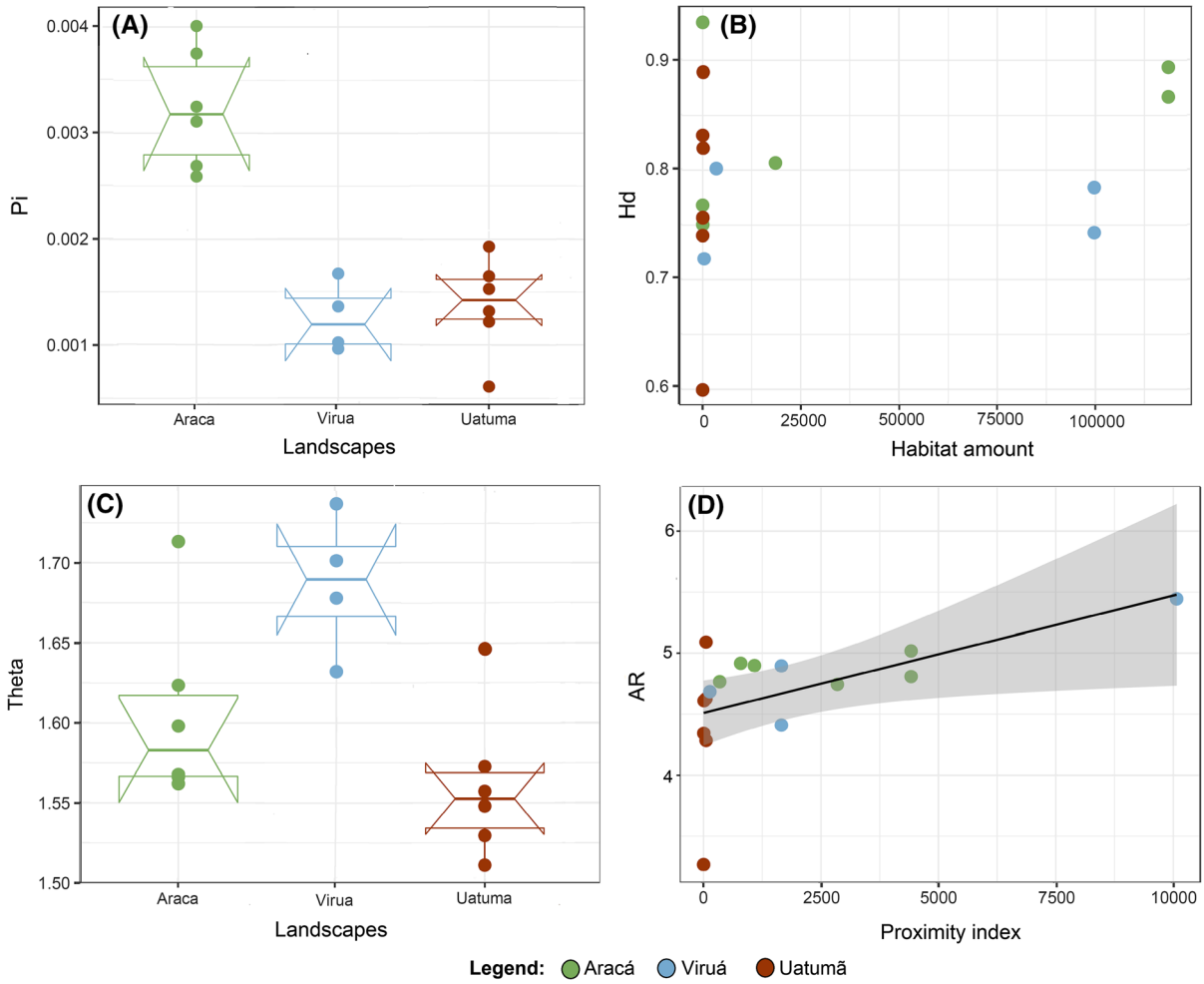

Fig. 4 Best models on the source of variation of mitochondrial **A** and **B** and microsatellite **C** and **D** genetic diversity among sites within landscapes (Aracá = green, Viruá = blue, Uatumã = red). **A** nucleotide diversity (P_i) based on ND2 is best explained by landscape; **B** haplotype diversity based on ND2 sequences and habitat amount in m^2 (but none of the predictor variables explained haplotype diversity; the constant model was selected as the best model). **C** Theta from microsatellite data is best explained by landscape, and **D** the microsatellite allelic diversity (A_R) is best explained by the Proximity index

the different patterns for mitochondrial *versus* microsatellite results at this scale could be due to incomplete lineage sorting between populations from Viruá and Uatumã, preventing detection of structure with mtDNA sequence data. Furthermore, mitochondrial data are limited for landscape scale genetic analysis because they lack enough signal for estimating local and recent demographic parameters, such as migration rate, and recent environmentally mediated divergence among populations (Pease et al. 2009). However, the combination of mitochondrial sequences and microsatellites provides complementarity and this approach has proved powerful in many applications (Wang 2011).

Genetic diversity and population structure: historical influences

The landscape with largest amount of habitat, Aracá, had the highest mitochondrial nucleotide (Pi) and haplotype (H_D) diversity, and two mtDNA populations recovered in population structure analyses (Figs. 1A, 2A). A similar pattern of high genetic diversity and population structure was found for another white-sand

Table 2 Variables used in model selection with their respective delta Δ AICc and weight values (AICw)

Model	Variables	Pi		H_D		Theta		A_R	
		ΔAICc	AICw	ΔAICc	AICw	ΔAICc	AICw	ΔAICc	AICw
M0	Constant	21	< 0.001	**0**	**0.5573**	5.4	0.049	2.5	0.1836
M1	Landscape	**0**	**0.7686**	3.6	0.093	**0**	**0.732**	4.3	0.0743
M2	Habitat amount	23.7	< 0.001	2.1	0.1981	7.7	0.016	5.2	0.0489
M3	Proximity	23.3	< 0.001	3	0.1226	6.7	0.025	**0**	**0.6499**
M4	Landscape + habitat amount	4.1	0.0986	7.1	0.0157	4.1	0.093	8.5	0.0092
M5	Landscape * habitat amount	13.2	0.001	12.5	0.0011	15.6	< 0.001	18.9	< 0.001
M6	Landscape + Proximity	3.5	0.1307	7.7	0.012	4.3	0.084	6.1	0.0315
M7	Landscape * Proximity	13.2	0.0011	16	< 0.001	13.7	< 0.001	11.1	0.0025

The best model (ΔAICc = 0) and the alternative plausible models (ΔAICc ≤ 2) are presented in bold. The genetic diversity variables for mitochondrial data are nucleotide diversity (Pi) and haplotype diversity and for the microsatellite data are Theta and NG. The independent variables are Habitat amount and Proximity index. The model used landscape as a fixed factor or as interacting variable

specialist bird, *Xenopipo atronitens,* in the same region (Capurucho et al. 2013). Thus, it is likely that historical landscape alterations, such as glacial cycles, may have caused past population isolation within the Aracá landscape.

The mtDNA data analysis suggests that population expansion of *E. ruficeps* started around 50,000 years before present (Fig. S2), in agreement with other Amazonian bird species from *campinas* (Capurucho et al. 2013; Matos et al. 2016), but contrasting with results obtained for *E. ruficeps* using both nuclear and mtDNA sequences (Ritter et al. 2021). This difference may be due to the lower mutation rates of nuclear markers (Allio et al. 2017), and increased sampling per locality used here. These historical demographic changes indicate that the populations of *E. ruficeps* may have started expanding in the last inter glacial, before the Last Glacial Maximum (LGM; Clark et al. 2009). When demography was estimated separately for each population cluster found in BAPS, the Aracá clusters, showed demographic expansion over the last 50,000 years (Fig. S3B), whereas the Viruá + Uatumã cluster showed constant population size (Fig. S3C), although the haplotype network showed a starburst pattern that is consistent with recent and rapid expansions (Slatkin and Hudson 1991). These results suggest that glacial cycles incurred variable impact in different regions of Amazonia and may explain the highest P_i, due to population expansion, in Aracá.

Studies on both northern (Carneiro Filho et al. 2002; Horbe et al. 2004; Teeuw and Rhodes 2004; Zular et al. 2019) and southern (Latrubesse 2002) Amazonian *campinas* indicate that this habitat responded to historical changes in climate, with the strongest signal detected in the north. An increase in sediment deposition, primarily from the Tepuis, and aeolian activity, on northern *campinas* (Teeuw and Rhodes 2004; Zular et al. 2019), could have increased connectivity among populations of white-sand specialist species by increasing the area and connectivity of campinas, and consequently increasing population size and genetic diversity, during drier climatic periods in the Aracá region. Contrastingly, the Viruá landscape currently has the highest Theta diversity. *Campina* patches in Viruá also have higher diversity of white-sand specialist bird species, possibly due to its proximity to other open habitat types such as the northern South America savannas (Fig. 1; Borges et al. 2016a; Capurucho et al. 2020a).

Estimated migration rates were asymmetrical, as found for other Amazonian birds (Capurucho et al. 2013; Menger et al. 2017), and we also found distinct values for historical and contemporary migration. Historical migration was higher between Uatumã and Viruá, with rates from Uatumã to Viruá three-fold higher than from Viruá to Uatumã. The Aracá landscape appears to be historically isolated from the other two landscapes. The historical isolation of Aracá may be explained by alterations to its overall size and/

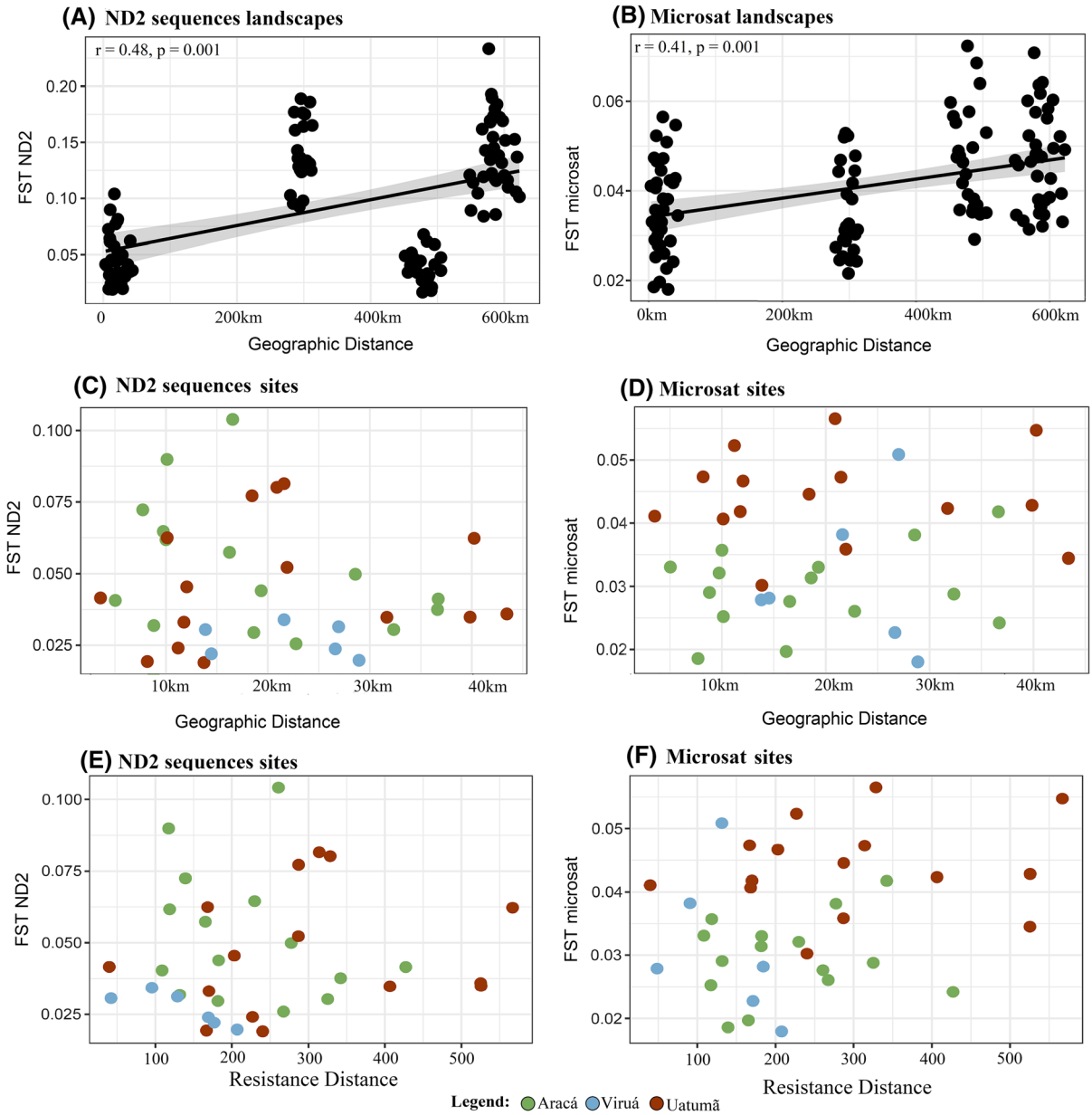

Fig. 5 Pairwise genetic distance (F_{ST}) and geographical distance relationship calculated with Mantel test. **A** F_{ST} from ND2 sequence data and **B** microsatellite data both plotted against the geographical distance between landscapes. **C** F_{ST} from ND2 sequence data and **D** microsatellite data both plotted against the geographical distance between sites inside each landscape. **E** F_{ST} from ND2 sequence data and **F** microsatellite data both plotted against the resistance distance between sites inside each landscape. The geographical distance is only significant between landscapes. **A** and **B** pairwise matrix for all sites and **C** to **F** the data from each landscape: green = Aracá; blue = Viruá and; red = Uatumã

or connectivity during the Pleistocene glacial cycles (Teeuw and Rhodes 2004) and by the establishment of the Branco River (Cremon et al. 2016). The Branco River is a white-water river that separates Aracá from Uatumã and Viruá and, together with its floodplains covered by seasonally flooded *várzea* vegetation, appear to impose a stronger resistance for *campina*'s specialist birds (Capurucho et al. 2013; Matos et al. 2016). Furthermore, as suggested by haplotype network and migration rates, both previously (Ritter

et al. 2021) and in this study, this river is also a barrier for *E. ruficeps*, which may have limited historical migration for Aracá populations. Analyses of sedimentary deposits and regional geomorphology suggested that a long segment of the Branco River was established in the Late Pleistocene (Cremon et al. 2016). The initial establishment of the Branco River at about 30 kya (Cremon et al. 2016) may have increased isolation of the Aracá population, but with gradual development of floodplain vegetation the barrier effect may be less pronounced since then. It is also possible that with the *terra-firme* canopy cover becoming less dense during past drier periods (Cowling et al. 2001), as hypothesized for northern Amazonia during the LGM (Häggi et al. 2017), the forested matrix surrounding *campinas* may have been more permeable than flooded forests along the Branco River, allowing for larger migration between Viruá and Uatumã, while Aracá remained isolated.

In summary, Pleistocene glacial cycles are a likely driver of population dynamics in of *E. ruficeps* through the increase of individual mobility across *terra-firme* forests in dry periods, while in the more isolated Aracá landscape, the continuous availability of the white-sand areas, even in wetter periods, may explain the higher genetic diversity. Genetic diversity patterns found for *E. ruficeps* are congruent with findings from other white-sand specialist birds (Capurucho et al. 2013; Matos et al. 2016), corroborating the idea that Pleistocene glacial cycles shaped current inter and intra-specific diversity (Rangel et al. 2018). This combined evidence from white-sand specialist birds suggests a dynamic interaction between closed canopy forests, open forests and non-forest/open vegetation areas (Cowling et al. 2001; Arruda et al. 2018), indicating that past climatic change deeply influenced Amazonian biogeographic history, and contradicting previous suggestions of a stable landscape in Amazonia during the Quaternary (Smith et al. 2014). This underscores the complex dynamics of *campina*'s habitats and highlights the potential impact of future climatic changes on *campinas*' biota. Many current models predict a drier future climate for Amazonia (Parsons 2020) with an increase of fires (Brando et al. 2020) leading to savannization. These future conditions would threaten species specialized in c*ampinas* due to both habitat degradation and increased competition with savannas' species, which are usually more tolerant to such conditions (Ritter et al. 2021).

Genetic diversity and population structure: contemporary influences

In contrast to the historical scenario, microsatellite data indicate that current migration occurs primarily from Uatumã and Viruá towards Aracá, with lower migration rates in all other directions. Asymmetrical gene flow arises due to more favorable dispersal conditions in one direction or due to source-sink dynamics across heterogeneous environments (e.g., Oswald et al. 2017; Moussy et al. 2018; Hauser et al. 2019). Aracá has the largest area of *campina* vegetation and is the most internally connected landscape. Furthermore, Aracá has in general the largest genetic diversity as measured here by three of the four indices, and in this context Aracá could function as a source population with a higher rate of emigration from Aracá towards the other populations. However, we found the opposite pattern, a higher migration rate towards Aracá, the largest and more connected population.

Considering the recent population expansion documented in Aracá over the last 50,000 years, in contrast to stability of population sizes in Uatumã and Viruá, it is possible that dispersal of individuals towards Aracá may be the result of emigration from small *campina* patches with little resource availability (e.g., Uatumã) or from landscapes that have been more affected by human impact (e.g., Viruá) with overall lower carrying capacity, but that are still able to maintain stable populations and thus are probably not sinks. Therefore, the asymmetrical gene flow in our study is most likely not consistent with a source-sink dynamic, and other mechanisms should be investigated. An increased cost for dispersing towards one direction, as observed along elevational gradients (Cheviron and Brumfield 2009) is unlikely in our study system, but it is possible that environmental fluctuations are less strong in northern Amazonia (Jimenez and Takahashi 2019), leading to more constant resource supply in Aracá (the northernmost landscape).

Landscape structure and landscape features have been shown to be important in shaping genetic diversity at the local scale for Amazonian vertebrates (e.g., Bates 2002; Capurucho et al. 2013; Menger et al. 2018; Silva et al. 2020). Here we show that allelic richness (A_R) decreased in more isolated *campina* patches, but with no effect of habitat amount, in contrast to other findings showing that habitat amount

best predicts genetic diversity and species diversity in white-sand specialist bird communities (Capurucho et al. 2013; Borges et al. 2016a).

This suggests that current local movements of *E. ruficeps*, at least to a certain degree, are shaped by the configuration of *campina* patches. However, for *Xenopipo atronitens*, another white-sand specialist bird, haplotype and nucleotide diversity increased with the amount of habitat available, with no effect of configuration (Capurucho et al. 2013). This difference may be explained by different species traits and habitat use patterns, since *X. atronitens* individuals also use white-sand patches more forested than *campinas* (also called *campinaranas*), and eventually exploit black-water floodplain forests (Oren 1981; Ridgely and Tudor 2009). In contrast, *E. ruficeps* is more restricted to *campina* vegetation (Borges et al. 2016b). Additionally, *E. ruficeps* has a lower handwing index (a proxy of species' dispersal capabilities) than *X. atronitens*, a trait that was found to be correlated with overall range size in white-sand specialist birds (Capurucho et al. 2020b). These differences in habitat use highlight the importance of considering species traits when addressing congruence in biogeographical scenarios (Papadopoulou and Knowles 2016). Thus, we conclude that white-sand specialist birds are affected by landscape structure, but different components of these landscapes influence movement patterns of different species and both habitat amount (for *X. atronitens*; Capurucho et al. 2013) and configuration (for *E. ruficeps*; this study) appear to be important for driving spatial patterns of genetic diversity of these white-sand specialist birds.

Genetic distance among landscapes increased with larger geographic distances in both mitochondrial and microsatellite data. Although significant genetic differentiation was found among most sampling sites within landscapes, no pattern of isolation by distance or resistance was observed. More refined studies on habitat permeability for white-sand vegetation birds are needed to develop more accurate isolation by resistance models. Our results suggest that although dispersal ability of *E. ruficeps* is at least to certain degree restricted by intervening vegetation types (Ritter et al. 2021), it is still greater than overall dispersal ability for most *terra-firme* forest birds (Menger et al. 2017, 2018), but dispersal ability of *E. ruficeps* is lower when compared to dispersal of savanna birds (Bates et al. 2003; Ritter et al. 2021). In a previous study comparing the population structure of *E. ruficeps* with its sister species *E. cristata*, it was evident that *E. cristata* populations, which occur in savannas, have less population structure, indicating higher mobility than *E. ruficeps* (Ritter et al. 2021). Furthermore, dispersal of *terra-firme* forest birds is generally limited by geographic distance (e.g. Menger et al. 2017, 2018), while typical Amazonian open area (savannas) bird species appear to have low population genetic structure, even at large geographic distances and across biogeographical barriers (Bates et al. 2003; Ritter et al. 2021).

Conclusions

Here, we infer population structure, genetic diversity and migration within *E. ruficeps,* an Amazonian white-sand specialist bird, in three landscapes, using both, mitochondrial and microsatellite data. Distinct population structure was found for the different markers used, indicating differences in historical and current patterns of connectivity among landscapes. Migration rates were asymmetrical and also indicated a distinct scenario in the past compared to current rates. Patch isolation within and among landscapes was important to explain spatial patterns of microsatellite genetic diversity (A_R). Geographical distance limited dispersal among but not within landscapes. These results suggest that both current landscape structure and the history of *campina* patches determine genetic diversity patterns of *campina* specialist birds. This study fosters our understanding of how biotic communities associated to white-sand patches are influenced by current and historical processes in Amazonia, contributing to predictions about how these communities will be affected by future climatic changes.

Acknowledgements We thank the Brazilian authorities, ICMBio (20524-3 ICMBio/MMA), CEUC-AM, PARNA Viruá, and RDS Uatumã (24597-2 ICMBio/MMA) for providing the collecting permits and logistical support, and Fundação Vitória Amazônica (FVA), and Instituto de Conservação e Desenvolvimento Sustentável do Amazonas (Idesam) for logistical support. Genetic sequencing was conducted at the Laboratório Temático de Biologia Molecular (LTBM-INPA). Genotyping data were gathered in the Pritzker Laboratory for Molecular Systematics and Evolution at the Field Museum of Natural History (FMNH). We thank Arielle Machado for reading an initial version of the manuscript and

Josué Azevedo for help with isolation by resistance analysis. We thank Gisiane Lima, João Capurucho, and Thiago Laranjeiras for answering the questionnaire about matrix resistance values.

Author contributions CC, CCR, CDR, and SHB designed the study. CDR and JM generated and analyzed the data. CDR wrote the manuscript with contributions of CC, CCR, CDB, JM, JPM, JB, and SHB.

Funding Open Access funding enabled and organized by Projekt DEAL. FAPESP and FAPEAM for financial support through the 'Fapesp-Fapeam' joint funding program (FAPESP 09/53365-0 granted to CC and JPM, and FAPEAM granted to CCR). CDR thanks the financial support from Alexander von Humboldt Foundation and CNPq (Conselho Nacional de Desenvolvimento Científico e Tecnológico—Brazil: 249064/2013-8). CCR is supported by a productivity fellowship from CNPq. C.D.B. is supported by the Swedish Research Council (2017-04980). During the execution of this study SHB received a grant from FAPEAM (Fixam program, Edital no. 017/2014).

Data availability GenBank accession ND2 sequences ID: 2304423. Microsatellite data is available in Ritter et al. (2014).

Code availability Not applicable.

Declarations

Conflict of interest The authors declare no conflicts or competing of interests.

Ethical approval ICMBio, CEUC-AM (20524-3 ICMBio/MMA), PARNA Viruá, and RDS Uatumã (24597-2 ICMBio/MMA) for collecting permits.

Consent to participate All authors declare to consent to participate of this study.

Consent for publication All authors declare to consent the publication of this study.

References

Adamack AT, Gruber B (2014) PopGenReport: simplifying basic population genetic analyses in R. Methods Ecol Evol 5:384–387

Adeney JM, Christensen NL, Vicentini A, Cohn-Haft M (2016) White-sand ecosystems in Amazonia. Biotropica 48:7–23

Allio R, Donega S, Galtier N, Nabholz B (2017) Large variation in the ratio of mitochondrial to nuclear mutation rate across animals: implications for genetic diversity and the use of mitochondrial DNA as a molecular marker. Mol Biol Evol 34:2762–2772

Anderson AB (1981) White-sand vegetation of Brazilian Amazonia. Biotropica 13:199–210

Antonelli A, Zizka A, Carvalho FA et al (2018) Amazonia is the primary source of Neotropical biodiversity. Proc Natl Acad Sci 115:6034–6039

Arruda DM, Schaefer CEGR, Fonseca RS, Solar RRC, Fernandes-Filho EI (2018) Vegetation cover of Brazil in the last 21 ka: new insights into the Amazonian refugia and Pleistocenic arc hypotheses. Glob Ecol Biogeogr 27(1):47–56. https://doi.org/10.1111/geb.12646

Avise JC (2009) Phylogeography: retrospect and prospect. J Biogeogr 36:3–15

Bates JM (2002) The genetic effects of forest fragmentation on five species of Amazonian birds. J Avian Biol 33:276–294

Bates JM, Tello JG, Silva JMC (2003) Initial assessment of genetic diversity in ten bird species of South American Cerrado. Stud Neotrop Fauna Environ 38:87–94

Beerli P (2009) How to use MIGRATE or why are Markov chain Monte Carlo programs difficult to use. Popul Genet Anim Conserv 17:42–79

Biomatters (2012) Geneious version 5.6. 5 created by Biomatters

Bolker B, Bolker MB (2017) Package 'bbmle', 1.0.20. https://rdrr.io/cran/bbmle/

Borges SH, Cornelius C, Moreira M et al (2016a) Bird communities in Amazonian white-sand vegetation patches: effects of landscape configuration and biogeographic context. Biotropica 48:121–131

Borges SH, Cornelius C, Ribas C et al (2016b) What is the avifauna of Amazonian white-sand vegetation? Bird Conserv Int 26:192–204

Brando PM, Soares-Filho B, Rodrigues L et al (2020) The gathering firestorm in southern Amazonia. Sci Adv 6:eaay1632

Capurucho JMG, Ashley MV, Tsuru BR et al (2020b) Dispersal ability correlates with range size in Amazonian habitat-restricted birds. Proc R Soc B 287:20201450

Capurucho JMG, Borges SH, Cornelius C et al (2020a) Patterns and processes of diversification in Amazonian white sand ecosystems: insights from birds and plants. In: Rull V, Carnaval AC (eds) Neotropical diversification: patterns and processes. Springer, Berlin, pp 245–270

Capurucho JMG, Cornelius C, Borges SH et al (2013) Combining phylogeography and landscape genetics of *Xenopipo atronitens* (Aves: Pipridae), a white sand campina specialist, to understand Pleistocene landscape evolution in Amazonia. Biol J Linn Soc 110:60–76

Carneiro Filho A, Schwartz D, Tatumi SH, Rosique T (2002) Amazonian paleodunes provide evidence for drier climate phases during the Late Pleistocene-Holocene. Quat Res 58:205–209

Cheng H, Sinha A, Cruz FW et al (2013) Climate change patterns in Amazonia and biodiversity. Nat Commun 4:1411

Cheviron ZA, Brumfield RT (2009) Migration-selection balance and local adaptation of mitochondrial haplotypes in rufous-collared sparrows (*Zonotrichia capensis*) along an elevational gradient. Evol Int J Org Evol 63:1593–1605

Clark PU, Dyke AS, Shakun JD et al (2009) The last glacial maximum. Science 325:710–714

Clement MJ, Snell Q, Walker P, et al (2002) TCS: estimating gene genealogies. In: ipdps. p 184

Converse PE, Kuchta SR, Roosenburg WM et al (2015) Spatiotemporal analysis of gene flow in Chesapeake Bay Diamondback Terrapins (*Malaclemys terrapin*). Mol Ecol 24:5864–5876

Corander J, Marttinen P, Sirén J, Tang J (2013) BAPS: Bayesian analysis of population structure. Finland University Helsinki

Costa FM, Terra-Araujo MH, Zartman CE et al (2020) Islands in a green ocean: spatially structured endemism in Amazonian white-sand vegetation. Biotropica 52:34–45

Cowling SA, Maslin MA, Sykes MT (2001) Paleovegetation simulations of lowland Amazonia and implications for neotropical allopatry and speciation. Quat Res 55:140–149

Crawley MJ (2013) The R book, Second edn. Wiley, West Sussex, p 942

Cremon ÉH, de Fátima RD, de Oliveira SA, Cohen MCL (2016) The role of tectonics and climate in the late quaternary evolution of a northern Amazonian River. Geomorphology 271:22–39

da Rocha DG, Kaefer IL (2019) What has become of the refugia hypothesis to explain biological diversity in Amazonia? Ecol Evol 9:4302–4309

Darriba D, Taboada GL, Doallo R, Posada D (2012) jModelTest 2: more models, new heuristics and parallel computing. Nat Methods 9:772

DiLeo MF, Wagner HH (2016) A landscape ecologist's agenda for landscape genetics. Curr Landsc Ecol Reports 1:115–126

Draper FC, Honorio Coronado EN, Roucoux KH et al (2018) Peatland forests are the least diverse tree communities documented in Amazonia, but contribute to high regional beta-diversity. Ecography (cop) 41:1256–1269

Drummond AJ, Rambaut A, Shapiro B, Pybus OG (2005) Bayesian coalescent inference of past population dynamics from molecular sequences. Mol Biol Evol 22:1185–1192

Drummond AJ, Suchard MA, Xie D, Rambaut A (2012) Bayesian phylogenetics with BEAUti and the BEAST 1.7. Mol Biol Evol 29:1969–1973

Earl DA (2012) STRUCTURE HARVESTER: a website and program for visualizing STRUCTURE output and implementing the Evanno method. Conserv Genet Resour 4:359–361

Evanno G, Regnaut S, Goudet J (2005) Detecting the number of clusters of individuals using the software STRUCTURE: a simulation study. Mol Ecol 14:2611–2620

Excoffier L, Laval G, Schneider S (2005) Arlequin (version 3.0): an integrated software package for population genetics data analysis. Evol Bioinf 1:117693430500100000

Fahrig L (1998) When does fragmentation of breeding habitat affect population survival? Ecol Modell 105:273–292

Fine PVA, García-Villacorta R, Pitman NCA et al (2010) A floristic study of the white-sand forests of Peru. Ann Missouri Bot Gard 97:283–305

Frankham R, Briscoe DA, Ballou JD (2002) Introduction to conservation genetics. Cambridge University Press, Cambridge

GBIF.org (2017) GBIF Occurrenc. https://doi.org/10.15468/dl.j6q8ht

Goudet J (2001) FSTAT, a program to estimate and test gene diversities and fixation indices, version 2.9.3. http://www2.unil.ch/popgen/softwares/fstat.htm

Goudet J, Jombart T (2015) hierfstat: estimation and tests of hierarchical F-statistics. R Packag version 004-22

Gruber B, Henle K (2008) Analysing the effect of movement on local survival: a new method with an application to a spatially structured population of the arboreal gecko Gehyra variegata. Oecologia 154:679–690

Gustafson EJ, Parker GR (1994) Using an index of habitat patch proximity for landscape design. Landsc Urban Plan 29:117–130

Häggi C, Chiessi CM, Merkel U et al (2017) Response of the Amazon rainforest to late Pleistocene climate variability. Earth Planet Sci Lett 479:50–59

Hale ML, Burg TM, Steeves TE (2012) Sampling for microsatellite-based population genetic studies: 25 to 30 individuals per population is enough to accurately estimate allele frequencies. PLoS One 7:e45170

Hansen MC, Potapov PV, Moore R et al (2013) High-resolution global maps of 21st-century forest cover change. Science 342:850–853

Hauser SS, Walker L, Leberg PL (2019) Asymmetrical gene flow of the recently delisted passerine black-capped vireo (*Vireo atricapilla*) indicates source-sink dynamics in central Texas. Ecol Evol 9:463–470

Horbe AMC, Horbe MA, Suguio K (2004) Tropical Spodosols in northeastern Amazonas State, Brazil. Geoderma 119:55–68

Hubisz MJ, Falush D, Stephens M, Pritchard JK (2009) Inferring weak population structure with the assistance of sample group information. Mol Ecol Resour 9:1322–1332

Hulce D, Li X, Snyder-Leiby T, Liu CSJ (2011) GeneMarker® genotyping software: tools to increase the statistical power of DNA fragment analysis. J Biomol Tech JBT 22:S35

Itescu Y (2019) Are island-like systems biologically similar to islands? A review of the evidence. Ecography (cop) 42:1298–1314

Jakobsson M, Rosenberg NA (2007) CLUMPP: a cluster matching and permutation program for dealing with label switching and multimodality in analysis of population structure. Bioinformatics 23:1801–1806

Jimenez JC, Takahashi K (2019) Tropical climate variability and change: impacts in the Amazon. Front Earth Sci 7:215

Latrubesse EM (2002) Evidence of Quaternary palaeohydrological changes in middle Amazônia: the Aripuanã-Roosevelt and Jiparaná" fans". ZEITSCHRIFT FUR Geomorphol Suppl 61–72

Leigh JW, Bryant D (2015) Popart: full-feature software for haplotype network construction. Methods Ecol Evol 6:1110–1116

Librado P, Rozas J (2009) DnaSP v5: a software for comprehensive analysis of DNA polymorphism data. Bioinformatics 25:1451–1452

Lovette IJ (2004) Mitochondrial dating and mixed support for the "2% rule" in birds. Auk 121:1–6

Manicacci D, Olivieri I, Perrot V et al (1992) Landscape ecology: population genetics at the metapopulation level. Landsc Ecol 6:147–159

Matos MV, Borges SH, d'Horta FM et al (2016) Comparative phylogeography of two bird species, *Tachyphonus phoenicius* (Thraupidae) and *Polytmus theresiae* (Trochilidae), specialized in Amazonian white-sand vegetation. Biotropica 48:110–120

McGarigal K, Cushman SA, Neel MC, Ene E (2002) FRAGSTATS: spatial pattern analysis program for categorical maps. Comput Softw Progr Prod by authors Univ Massachusetts, Amherst Available Follow web site www.umass.edu/landeco/research/fragstats/fragstats

McRae BH (2006) Isolation by resistance. Evolution 60:1551–1561

Menger J, Henle K, Magnusson WE et al (2017) Genetic diversity and spatial structure of the Rufous-throated Antbird (*Gymnopithys rufigula*), an Amazonian obligate army-ant follower. Ecol Evol 7:2671–2684

Menger J, Unrein J, Woitow M et al (2018) Weak evidence for fine-scale genetic spatial structure in three sedentary Amazonian understorey birds. J Ornithol 159:355–366

Moussy C, Arlettaz R, Copete JL et al (2018) The genetic structure of the European breeding populations of a declining farmland bird, the ortolan bunting (*Emberiza hortulana*), reveals conservation priorities. Conserv Genet 19:909–922

Myster RW (2016) The physical structure of forests in the Amazon Basin: a review. Bot Rev 82:407–427

Oksanen J, Blanchet FG, Kindt R, et al (2010) Vegan: community ecology package. R package version 1.17-4. http://cran.r-project.org

Oren DC (1981) Zoogeographic analysis of the white sand campina avifauna of Amazonia. PhD Thesis. Harvard University

Oswald JA, Overcast I, Mauck WM III et al (2017) Isolation with asymmetric gene flow during the nonsynchronous divergence of dry forest birds. Mol Ecol 26:1386–1400

Papadopoulou A, Knowles LL (2016) Toward a paradigm shift in comparative phylogeography driven by trait-based hypotheses. Proc Natl Acad Sci 113:8018–8024

Parsons LA (2020) Implications of CMIP6 projected drying trends for 21st century Amazonian drought risk. Earth's Futur 8:e2020EF001608

Pease KM, Freedman AH, Pollinger JP et al (2009) Landscape genetics of California mule deer (*Odocoileus hemionus*): the roles of ecological and historical factors in generating differentiation. Mol Ecol 18:1848–1862

Prance GT (1996) Islands in Amazonia. Philos Trans R Soc Lond Ser B Biol Sci 351:823–833

Press E (2005) Linear Referencing in ArcGIS: ArcGIS 9. Esri Press

Pritchard JK, Stephens M, Donnelly P (2000) Inference of population structure using multilocus genotype data. Genetics 155:945–959

QGIS.org (2021) QGIS Geographic Information System. QGIS Association, 3.6.2. http://www.qgis.org

R Core Team (2015) R: a language and environment for statistical computing

Rambaut A, Drummond AJ (2007) Tracer v1. 4: MCMC trace analyses tool

Rangel TF, Edwards NR, Holden PB et al (2018) Modeling the ecology and evolution of biodiversity: biogeographical cradles, museums, and graves. Science 361:eaar5452

Raymond M, Rousset F (1995) Population genetics software for exact test and ecumenicism. J Hered 86:248–249

Rheindt FE, Norman JA, Christidis L (2008) Phylogenetic relationships of tyrant-flycatchers (Aves: Tyrannidae), with an emphasis on the elaeniine assemblage. Mol Phylogenet Evol 46:88–101

Ridgely RS, Tudor G (2009) Field guide to the songbirds of South America: the passerines. University of Texas Press

Ritter CD, Coelho LA, Capurucho JMG et al (2021) Sister species, different histories: comparative phylogeography of two bird species associated with Amazonian open vegetation. Biol J Linn Soc. https://doi.org/10.1093/biolinnean/blaa167

Ritter CD, Figueiredo CMÉ, Gubili C et al (2014) Isolation and characterization of seventeen polymorphic microsatellite DNA markers from *Elaenia ruficeps* (Aves: Tyrannidae). Conserv Genet Resour. https://doi.org/10.1007/s12686-014-0273-x

Ritter CD, Zizka A, Roger F et al (2018) High-throughput metabarcoding reveals the effect of physicochemical soil properties on soil and litter biodiversity and community turnover across Amazonia. PeerJ 2018:e5661

Ronce O (2007) How does it feel to be like a rolling stone? Ten questions about dispersal evolution. Annu Rev Ecol Evol Syst 38:231–253

Rosenberg NA (2004) DISTRUCT: a program for the graphical display of population structure. Mol Ecol Notes 4:137–138

Rousset F (2008) genepop'007: a complete re-implementation of the genepop software for Windows and Linux. Mol Ecol Resour 8:103–106

Silva SM, Ferreira G, Pamplona H, et al (2020) Effects of landscape heterogeneity on population genetic structure and demography of Amazonian phyllostomid bats. Mammal Res 1–9

Silva SM, Peterson AT, Carneiro L et al (2019) A dynamic continental moisture gradient drove Amazonian bird diversification. Sci Adv 5:eaat752

Slatkin M, Hudson RR (1991) Pairwise comparisons of mitochondrial DNA sequences in stable and exponentially growing populations. Genetics 129:555–562

Sorenson MD, Ast JC, Dimcheff DE et al (1999) Primers for a PCR-based approach to mitochondrial genome sequencing in birds and other vertebrates. Mol Phylogenet Evol 12:105–114

Tautz D (1989) Hypervariability of simple sequences as a general source for polymorphic DNA markers. Nucleic Acids Res 17:6463–6471

Teeuw RM, Rhodes EJ (2004) Aeolian activity in northern Amazonia: optical dating of Late Pleistocene and Holocene palaeodunes. J Quat Sci Publ Quat Res Assoc 19:49–54

Tuomisto H, Van Doninck J, Ruokolainen K et al (2019) Discovering floristic and geoecological gradients across Amazonia. J Biogeogr 46:1734–1748

van Etten J (2017) R package gdistance: distances and routes on geographical grids

Van Houtan KS, Pimm SL, Halley JM et al (2007) Dispersal of Amazonian birds in continuous and fragmented forest. Ecol Lett 10:219–229

Wang IJ (2011) Choosing appropriate genetic markers and analytical methods for testing landscape genetic hypotheses. Mol Ecol 20:2480–2482

Wang X, Edwards RL, Auler AS et al (2017) Hydroclimate changes across the Amazon lowlands over the past 45,000 years. Nature 541:204

Weir BS, Cockerham CC (1984) Estimating F-statistics for the analysis of population structure. Evolution (N Y) 38:1358–1370

Weir JT, Schluter D (2008) Calibrating the avian molecular clock. Mol Ecol 17:2321–2328

Wilson GA, Rannala B (2003) Bayesian inference of recent migration rates using multilocus genotypes. Genetics 163:1177–1191

Wright S (1943) Isolation by distance. Genetics 28:114

Zular A, Sawakuchi AO, Chiessi CM et al (2019) The role of abrupt climate change in the formation of an open vegetation enclave in northern Amazonia during the late Quaternary. Glob Planet Change 172:140–149